

Dispersive regime of spectral compression

A.A. Kutuzyan, T.G. Mansuryan, G.L. Yesayan, R.S. Hakobyan, L.Kh. Mouradian

Abstract. The role of the group velocity dispersion in the spectral compression of subpicosecond laser pulses is analysed based on numerical and experimental studies. It is shown that the group velocity dispersion in an optical fibre can substantially change the physical pattern of the spectral compression process.

Keywords: ultrashort laser pulse, spectral compression, group velocity dispersion.

1. Introduction

Progress in the field of generation of ultrashort pulses stimulates the studies of self-phase modulation (SPM) and cross-phase modulation of radiation aimed at solving a number of problems related to the control and recording of femtosecond optical signals [1–5]. Of special interest from this point of view is the spectral compression of radiation based on the nonlinear SPM and cross-phase modulation of initially chirped ultrashort pulses [5–14]. Spectral compression was applied in the last decade in the optics of ultrafast processes and laser physics for recording the time envelope of the amplitude and phase of ultrashort pulses by means of the Fourier transform [5], fine frequency tuning of radiation [5], nonlinear optical filtration of noise [11], generation of dark solitons [13], in the *D*-scan method developed similarly to the *z*-scan method [14], for the transfer of ultrashort pulses over long distance without distortions [15], generation of high-power transform-limited ultrashort pulses in single-mode fibres (SMFs) with amplification [16], etc.

A system for the spectral compression of ultrashort pulses proposed in [7] consists of a dispersive delay line (DDL) and a SMF. Ultrashort pulses are stretched in the DDL with the anomalous dispersion, by acquiring a negative chirp. The further self-action of ultrashort pulses in the SMF with the Kerr nonlinearity leads to the compensation of the chirp and spectral compression due to SPM. The spectral compression of picosecond and femtosecond pulses was experimentally observed for the first time in [8] and [9], respectively. In the general case, the propagation of ultrashort pulses in SMFs should be studied taking into account, along with SPM, the second- and third-

order dispersion and the nonstationarity and relaxation of nonlinearity, which can cause the deformation of the time and spectral profiles of ultrashort pulses and formation of the shock waves of the time envelope [10, 17]. The study of the influence of these factors on spectral compression will make it possible to propose recommendations for the development of experimental spectral-compression schemes for specific applications.

In this paper, we studied the influence of the second-order dispersion in a SMF on the spectral compression of ultrashort pulses in the DDL–SMF system.

2. Mathematical description

Unlike [8, 10], we separate the contributions from different physical factors to the spectral compression process. First, the Kerr nonlinearity in a silica fibre has the electronic nature and its relaxation time is several femtoseconds [17]. Therefore, the influence of the nonlinearity relaxation on the spectral compression of ultrashort pulses of duration (FWHM) $\Delta t \sim 100$ fs can be neglected. The wave nonstationarity determined by the ratio of the light wave period to the pulse duration ($\sim 10^{-2}$) can be also neglected for such ultrashort pulses in the wavelength region $\lambda \sim 1$ μm [17]. The contributions of the second-order dispersion [group velocity dispersion (GVD)] and third-order dispersion in silica SMFs for ultrashort pulses with parameters indicated above become substantial at distances $L_d^{(2)} = \tau_0^2/k_2 \sim 0.1$ m and $L_d^{(3)} = 2\tau_0^3/k_3 \sim 10$ m, respectively, where τ_0 is the initial half-width of the ultrashort pulse at the 1/e level of the pulse intensity maximum and $k_j = |d^j k/d\omega^j|$ is the absolute value of the *j*th derivative of the wave number *k* with respect to frequency at the central radiation frequency ω_0 [17]. Thus, the use of fibres of length $f \sim 1$ m in the case of ~ 1 - μm femtosecond pulses allows one to consider only the influence of the second-order dispersion on spectral compression and describe this process by using the nonlinear Schrödinger equation [17]

$$i \frac{\partial \Psi}{\partial \zeta} = -\frac{1}{2} \frac{\partial^2 \Psi}{\partial \eta^2} + R |\Psi|^2 \Psi. \quad (1)$$

Here, $\Psi(\zeta, \eta)$ is the slowly varying amplitude normalised to its peak value at the input to the system; $\zeta = z/L_d$ is the dimensionless distance; $\eta = (t - z/u)/\tau_0$ is the running time; *z* is the spatial coordinate; $L_d \equiv L_d^{(2)}$; *u* is the group velocity; $R = L_d/L_{\text{nl}}$ is the nonlinearity parameter; $L_{\text{nl}} = (kn_2 I_0)^{-1}$ is the SPM length; n_2 is the nonlinearity coefficient; I_0 is the peak value of the input radiation intensity. The first term in the right-hand side of Eqn (1) describes dispersion effects and the second one describes nonlinear self-action effects. The DDL can be described by Eqn (1)

A.A. Kutuzyan, T.G. Mansuryan, G.L. Yesayan, R.S. Hakobyan, L.Kh. Mouradian Faculty of Physics, Yerevan State University, A. Manoogian St. 1, 0025 Yerevan, Armenia; e-mail: lmouradian@ysu.am

Received 17 September 2007; revision received 11 December 2007
Kvantovaya Elektronika 38 (4) 383–387 (2008)
Translated by M.N. Sapozhnikov

with $R = 0$ and $\zeta = -Z$, where Z is the dimensionless DDL length normalised to the dispersive length L_d [for the DDL, $(k_2^{(d)})$ should be used instead of $(k_2^{(f)})$ for the SMF].

3. Numerical studies

Equation (1) was solved numerically by the method of splitting over physical factors by using the algorithm of the fast Fourier transform on a dispersive step [18]. The temporal intensity distributions $I(\eta) = |\Psi(\eta)|^2$, frequencies $\Omega(\eta)$ (chirp), and the spectral power density $S(\Omega) = |F(\Omega)|^2$ of ultrashort pulses were determined at the outputs of the spectral-compression system and DDL depending on the radiation power specified by the parameter R [$F(\Omega)$ is the Fourier transform of the complex amplitude $\Psi(\eta)$ and $\Omega = (\omega - \omega_0)\tau_0$ is the dimensionless frequency].

Figure 1 presents the results of numerical studies demonstrating the dependence of $S(\Omega)$ at the output from the system on R in the nonlinear regime (in which the role of dispersion is insignificant) and in the dispersive regime (where the role of dispersion is considerable). The DDL length was $Z = 3$ (Figs 1a, b), 6 (Figs 1c, d), and 12 (Figs 1e, f) and the SMF length was $\zeta = 3$. One can see that the spectrum is compressed with increasing R , its compression becomes maximal, and then energy is transferred from the central peak to spectral satellites. A comparison of the dispersive and nonlinear regimes at different DDL lengths shows that the GVD in the SMF plays a significant role when Z is small, whereas for $Z = 12$ the GVD contribution is negligible. The influence of the GVD in the region of maximal compression is manifested in the smoothing of the dynamic pattern of spectral compression.

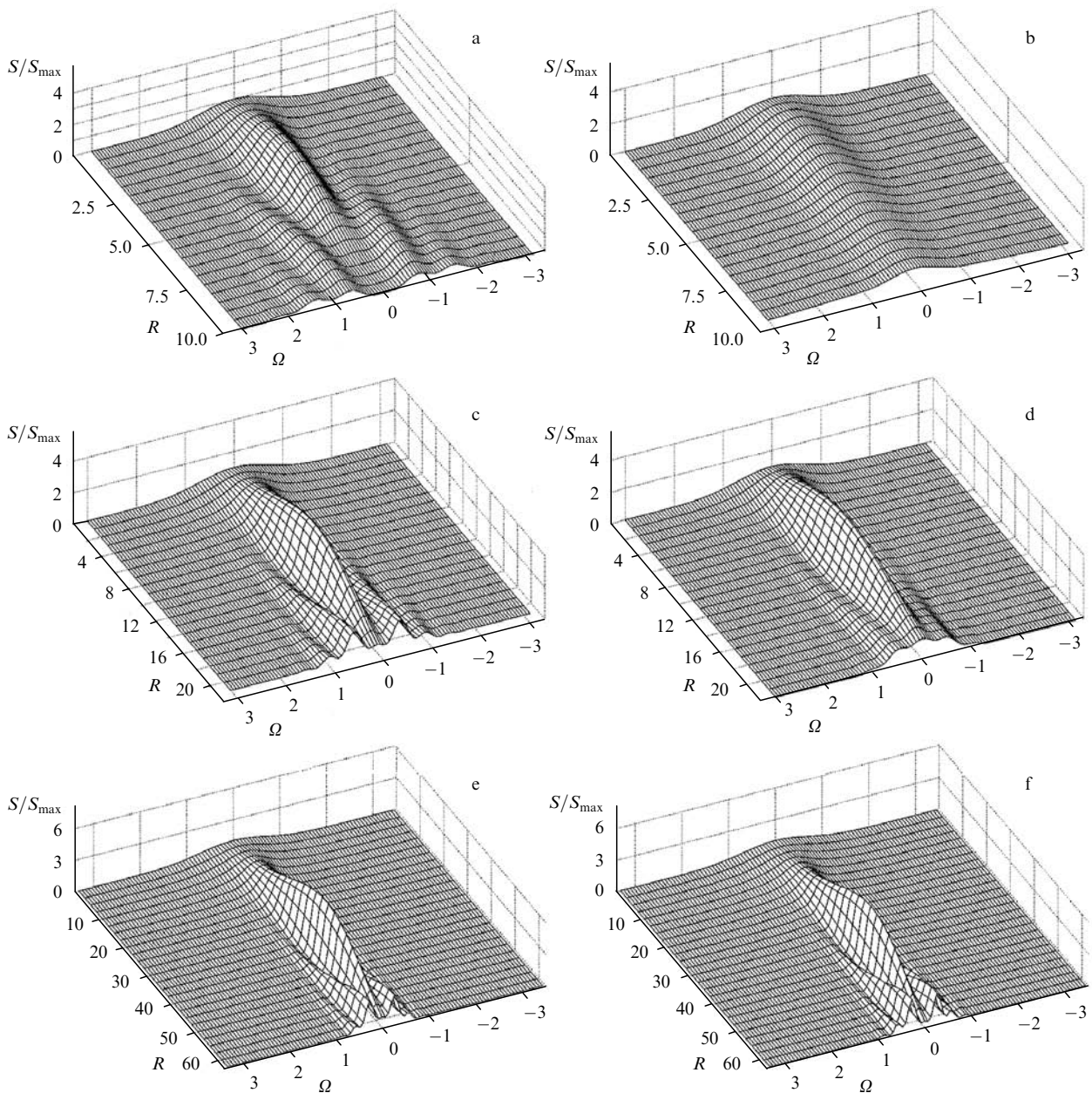


Figure 1. Spectral power density $S(\Omega)$ of an ultrashort pulse, normalised to its maximum S_{\max} for the initial pulse, at the output from the spectral compression system as a function of the nonlinearity parameter R in the dispersive (a, c, e) and nonlinear (b, d, f) regimes for $\zeta = 3$, $Z = 3$ (a, b), 6 (c, d), and 12 (e, f).

sion: spectral satellites in the dispersive regime are less pronounced compared to the dispersive regime and the maximum spectral compression is achieved at lower values of R . Note that $R\zeta \sim I_0 f$ in the nonlinear regime is an invariant of the process [17] and patterns in Figs 1a, c, e can be interpreted as the evolution of the emission spectrum along the SMF for the specified I_0 .

Figure 2 presents the time profile of the radiation intensity, chirp, and spectral power density for the values of R optimal for spectral compression in the nonlinear and dispersive regimes. The dependences are calculated for DDL lengths $Z = 3$ (Figs 2a, d, g), 6 (Figs 2b, e, h), and 12 (Figs 2c, f, i) and the SMF length $\zeta = 3$ by using the values of R providing the maximum spectral compression. One can see from Figs 2a, d, g that at small DDL lengths ($Z = 3$), i.e. for $d < fk_2^{(f)}/k_2^{(d)}$ (d is the DDL length), the normal GVD in the optical fibre leads to the temporal compression of ultrashort pulses, preventing thereby the spectral compression. In another limiting case of large DDL lengths ($Z = 12$), i.e. for $d \gg fk_2^{(f)}/k_2^{(d)}$, which is presented in Figs 2c, f, i, the contribution of the GVD in the fibre is insignificant, and the chirp cancellation and spectral compression occur virtually in the same way as in the nonlinear

regime. Figures 2b, e, h ($Z = 6$) illustrate the combined action of the GVD and Kerr nonlinearity resulting in the deformation of the time envelope $I(\eta)$ tending to acquire a rectangular shape. Unlike the nonlinear regime, in the dispersive regime the chirp is compensated for the entire ultrashort pulse (Fig. 2e). The compressed spectrum has weak sidebands and is described by the function $\text{sinc}\Omega$, which is the Fourier transform of a rectangular function. The formation of an ultrashort pulse with the rectangular envelope also determines the degree of spectral compression $C \equiv \Delta\omega_0/\Delta\omega = \tau/(2\tau_0)$ because in the case of the complete compensation of the chirp, $\Delta\omega\tau = 2$ for such pulses (where $\Delta\omega$ is the half-width of the spectral power density at the 1/e level).

Simulations performed for different values of Z and ζ show that ultrashort pulses with a rectangular envelope are formed for $Z/\zeta \sim 2$, i.e. for $d \sim 2fk_2^{(f)}/k_2^{(d)}$, and in this case the spectral-compression regime is achieved which provides the efficient generation of transform-limited ultrashort pulses. Note that the generation of ultrashort pulses with the rectangular envelope in the SMF due to the combined action of the GVD and Kerr nonlinearity upon optimisation of the temporal compression of ultrashort pulses was

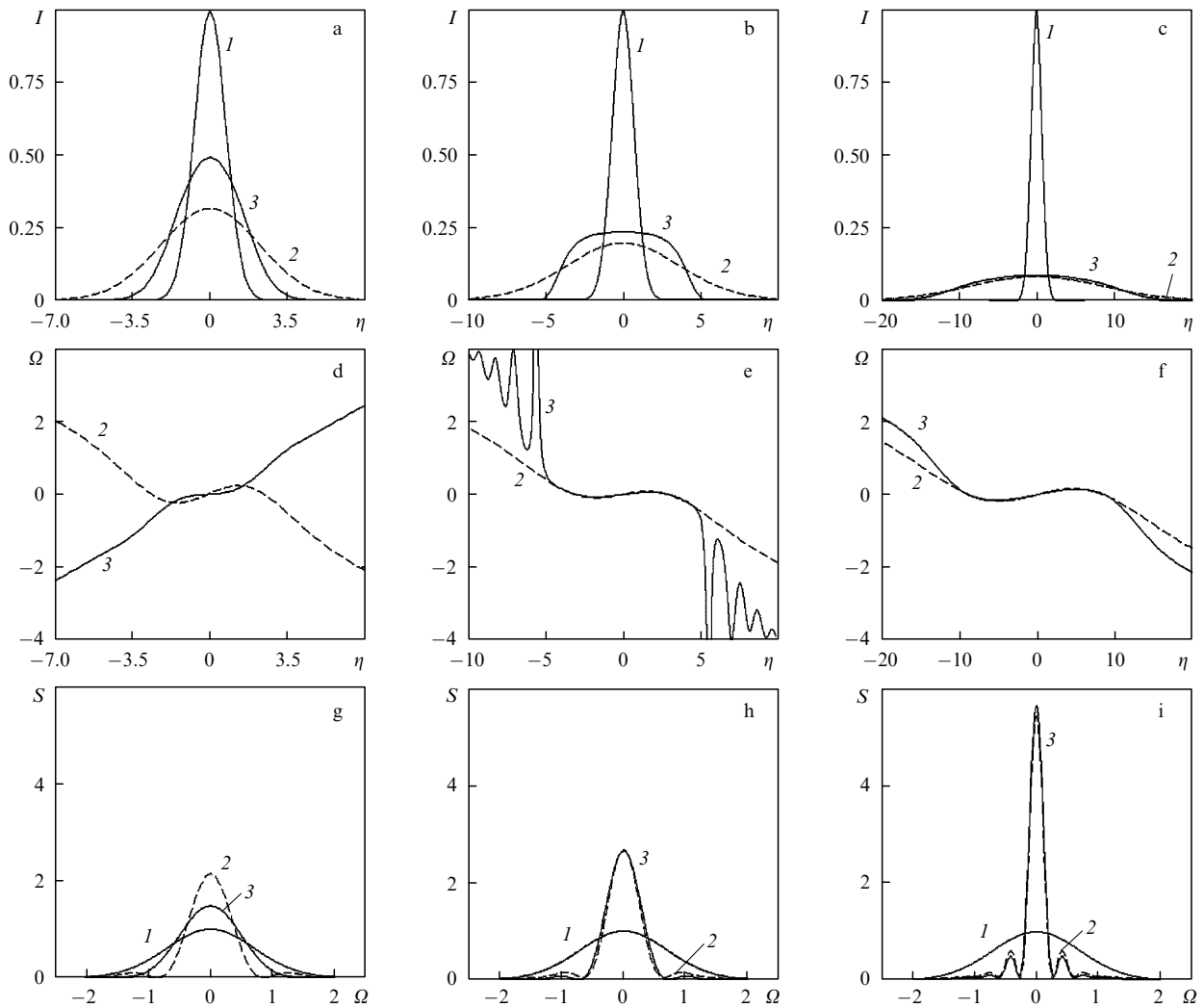


Figure 2. Time intensity profile I (a–c), chirp Ω (d–f), and spectral power density S (g–i) at the input to the spectral compression system (1) and at its output in the nonlinear (2) and dispersive (3) regimes for $\zeta = 3$ and $Z = 3$, $R = 2$ (3) and 3.5 (2) (a, d, g); $Z = 6$, $R = 9$ (3) and 12 (2) (b, e, h); and $Z = 12$, $R = 39$ (3), and 40 (2) (c, f, i).

observed at lengths $\zeta \simeq 1.8R^{-1/2}$ [17]. A simple generalisation of this relation taking into account the stretching of ultrashort pulses in the DDL does not correspond to the results presented. This could be expected because the influence of the GVD is caused not only by the ultrashort pulse duration but also by the radiation spectrum and phase.

4. Experiment

The experimental setup consisted of a femtosecond Ti : sapphire laser (Coherent Verdi10-Mira 900F), a spectral compressor, and an Ando AQ6315 spectrum analyser. The laser emitted ~ 800 -nm pulses at a pulse repetition rate of 76 MHz, the spectral width was $\Delta\lambda \sim 6$ nm. The pulse FWHM duration was $\Delta t \leq 150$ fs ($\Delta t \simeq 1.67\tau_0$) and the average output power was $p \sim 1.5$ W. The spectral

compressor consisted of a DDL (a pair of dispersive prisms with a reversing mirror) and a SMF with the mode field diameter $5.6 \mu\text{m}$, the nonlinearity coefficient $n_2 = 3.2 \times 10^{-16} \text{ cm}^2 \text{ W}^{-1}$, and the GVD $k_2^{(f)} = 4.6 \times 10^4 \text{ fs}^2 \text{ m}^{-1}$.

Figure 3 presents the spectral profiles of the output ultrashort pulses of the spectral-compression system obtained for different average radiation powers in the SMF of length $f = 0.95$ m and the distance between prisms $d = 3$ m. The dashed curves are the results of numerical simulations obtained for parameters of radiation and the DDL–SMF system corresponding to the experiment ($Z = 10$, $\zeta = 6.6$). At low radiation powers ($p < 1$ mW), the linear propagation of ultrashort pulses is observed, the output spectrum coinciding with the input spectrum of width $\Delta\lambda_{\text{in}} = 6$ nm (Fig. 3a). As the radiation power is increased, spectral compression occurs down to

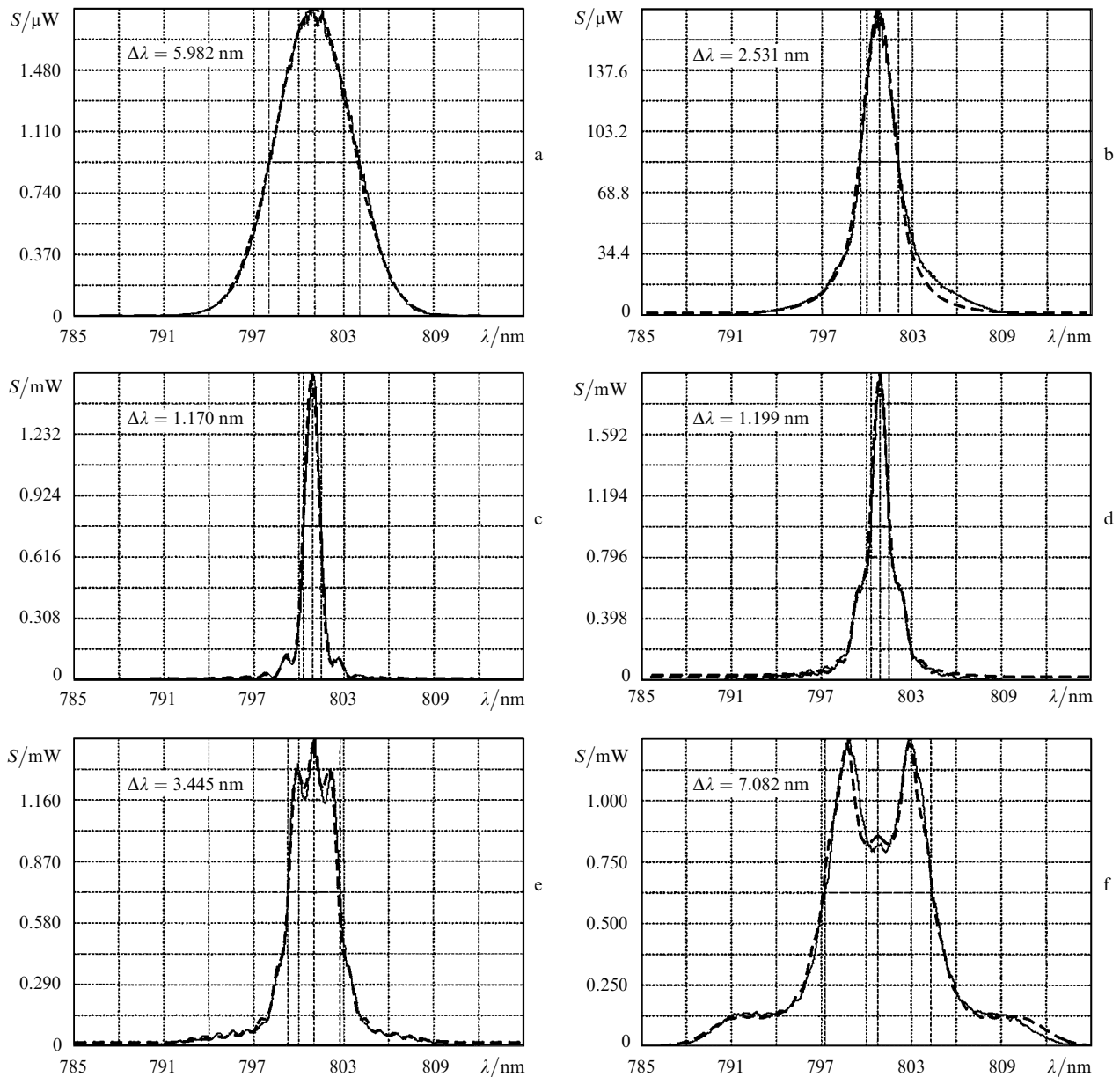


Figure 3. Spectral power density of ultrashort pulses at the output of the spectral compression system for average radiation powers coupled into the SMF $p = 200.5 \mu\text{W}$ (a), 10.3 (b), 37.51 (c), 71.7 (d), 99.6 (e), and 170.1 mW (f). The dashed curves are calculations, solid curves are obtained experimentally.

$\Delta\lambda_{\text{out}} = 1.2 \text{ nm}$ ($p \sim 37.5 \text{ mW}$) (Figs 3b, c). As the radiation power is further increased, the spectrum broadens. In this case, the shape of the spectra differs from the typical shape of SPM spectra, which suggests that the GVD plays an important role. Note that the broadened spectra are symmetric, which suggests that the influence of high-order dispersion and nonlinear effects on spectral compression is absent at these parameters of the system.

Figure 4 presents the generalised experimental results obtained for different radiation parameters and different SMFs. Figure 4a shows the dependence of the spectral compression coefficient C on the average radiation power in the SMF for $d = 3 \text{ m}$ and $f = 0.95 \text{ m}$. One can see that experimental results (circles) are in good quantitative agreement with calculations (solid curves). The power dependence of the spectral compression coefficient calculated in the absence of GVD is also presented (dashed curves). Figure 4b shows the corresponding results for $d = 1.03 \text{ m}$ and $f = 0.21 \text{ m}$ ($Z = 2.9$, $\zeta = 1.5$).

One can see from Fig. 4 that the influence of the GVD in the optical fibre can significantly change the transformation of the shape and spectrum of ultrashort pulses. For DDL lengths $d \sim 2fk_2^{(f)}/k_2^{(d)}$, the dispersive regime of spectral compression is efficiently realised (Figs 2b, e, h) in which the time envelope of ultrashort pulses at the spectral compressor output acquires a rectangular shape. In this case, the ultrashort pulse duration is virtually determined by its stretching in the DDL: $\tau \approx (k_2^{(d)}/\tau_0)d$. For DDL lengths $d < 2fk_2^{(f)}/k_2^{(d)}$, the time compression of ultrashort pulses in the SMF blocks the spectral compression (Figs 2a, d, g),

and the pulse duration at the output of the DDL–SMF system becomes smaller than its duration at the output from the DDL. For $d \gg 2fk_2^{(f)}/k_2^{(d)}$, the influence of the GVD is insignificant and the physical pattern of spectral compression is similar to that in the nonlinear regime (Figs 2c, f, i).

5. Conclusions

We have found that, along with the self-phase modulation, the GVD in SMFs plays a considerable role in the spectral compression of femtosecond pulses. The influence of GVD depends on the parameters of the spectral compression system, namely, on the relation between the lengths of the SMF and DDL measured in dispersive lengths:

(i) for DDL lengths smaller than the SMF length, the recompression of ultrashort pulses in the SMF caused by GVD blocks the spectral compression;

(ii) for DDL lengths greatly exceeding the SMF length, the role of GVD becomes insignificant;

(iii) for DDL lengths comparable with the double SMF length, the efficient dispersive spectral compression regime is achieved in which transform-limited ultrashort pulses with a rectangular time envelope are generated in the region of the maximum spectral compression.

The results obtained in the paper can be used in spectral compression schemes for controlling parameters of optical signals and their recording.

Acknowledgements. This work was supported by the NATO Sfp 978027 Grant.

References

1. Vampouille M., Marty J., Froehly C. *IEEE J. Quantum Electron.*, **22**, 192 (1986).
2. Wang Q.Z., Lui Q.D., Lui D., Ho P.P., Alfano R.R. *J. Opt. Soc. Am. B*, **11**, 1084 (1994).
3. Boyer G.R., Lachger M., et al. *J. Opt. Soc. Am. B*, **11**, 1451 (1994); Spenser P.S., Score K.A. *J. Opt. Soc. Am. B*, **12**, 67 (1995).
4. Niberring E.T.J., Franco M.A., Prade B.S., et al. *Opt. Commun.*, **119**, 479 (1995).
5. Mouradian L.Kh., Froehly C., Louradour F., Barthelemy A. *IEEE J. Quantum Electron.*, **36**, 795 (2000).
6. Kane D.J., Trebino R. *Opt. Lett.*, **18**, 823 (1993); Lingwei Guo, Changhe Zhou. *Opt. Commun.*, **260**, 140 (2006).
7. Markaryan N.L., Muradyan L.Kh., et al. *Kvantovaya Elektron.*, **18**, 865 (1991) [*Sov. J. Quantum Electron.*, **21**, 783 (1991)].
8. Planas S.A., Pires Mansur N.L., Brito Cruz C.H., Frangnito H.L. *Opt. Lett.*, **18**, 669 (1993).
9. Zograbyan A.V., Muradyan L.Kh. *Kvantovaya Elektron.*, **22**, 695 (1995) [*Quantum Electron.*, **25**, 668 (1995)]; *J. Contemp. Phys.*, **29**, 246 (1992).
10. Oberthaler M., Hopfel R.A. *Appl. Phys. Lett.*, **63**, 1017 (1993).
11. Margarian N.L., Mouradian L.Kh., Papazian T.A., et al. *J. Contemp. Phys.*, **27**, 128 (1992).
12. Markaryan N.L., Muradyan L.Kh., et al. *Kvantovaya Elektron.*, **22**, 1111 (1995) [*Quantum Electron.*, **25**, 1076 (1995)].
13. Kutuzyan A.A., Mansuryan T.G., Kirakosyan A.A., Mouradian L.Kh. *Proc. SPIE Int. Soc. Opt. Eng.*, **5135**, 156 (2003).
14. Louradour F., Lopez Lago E., Couderc V., Barthelemy A., Mouradian L. *Proc. ECIO'99* (Turin, 1999) p. 103.
15. Clark S.W., Ilday F.O., Wise F.W. *Opt. Lett.*, **26**, 17 (2001).
16. Schreiber T., Liem A., Röser F., Zellmer H., Tünnermann A., et al. *Proc. SPIE Int. Soc. Opt. Eng.*, **5709**, 32 (2005).
17. Akhmanov S.A., Vysloukh V.A., Chirkin A.S. *Optika femtosekundnykh lazernykh impul'sov* (Optics of Femtosecond Laser Pulses) (Moscow: Nauka, 1988).

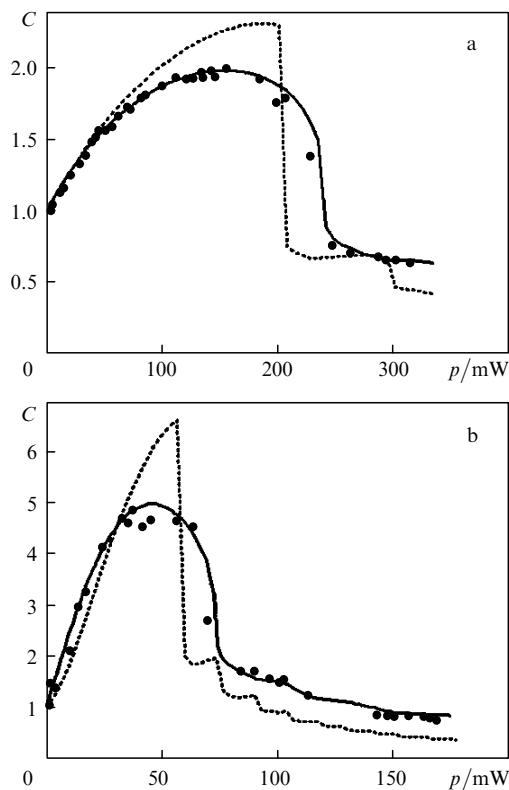


Figure 4. Dependences of the spectral compression coefficient C on the average radiation power coupled into the SMF for $d = 3 \text{ m}$, $f = 0.95 \text{ m}$ ($Z = 10$, $\zeta = 6.6$, $R = 0 - 53$) (a) and $d = 1.03 \text{ m}$, $f = 0.21 \text{ m}$ ($Z = 2.9$, $\zeta = 1.5$, $R = 0 - 25$) (b). Circles are experimental data, solid curves are calculated, and dashed curves are calculated in the absence of GVD.